

## A Real Time Visual Inspection System for Rail Flaw Detection

Gimy Joy<sup>1</sup> Jyothis R.L<sup>2</sup>

<sup>1</sup> PG Scholar, Department of CSE, College of Engineering, Karunagapally.

<sup>2</sup> Asst. Professor, Department of CSE, College of Engineering, Karunagapally.

<sup>1</sup>[gimyjoy@gmail.com](mailto:gimyjoy@gmail.com)

---

**ABSTRACT:** Rail inspection is an important task in railway maintenance. The speed and loads of trains have been increasing greatly in recent years, and these factors inevitably raise the risk of producing rail defects. Mainly the discrete surface defects impact the riding quality and safety of a railway system. However, it is a challenge to inspect such defects in a vision system because of illumination inequality and the variation of reflection property of rail surfaces. This project presents a real-time VIS for discrete surface defects of rail heads. VIS comprises the Image Acquisition Subsystem (IAS) and the image analysis subsystem. IAS acquires gray rail images for the surface of a rail head, and the latter processes rail images and detects possible defects. This paper propose the Local Normalization(LN) method to enhance the distinction between defects and background in a rail image, considering illumination inequality and the variation of reflection property of rail surfaces. VIS first acquires a rail image by the image acquisition system, and then, it cuts the sub image of rail. Track by the track extraction algorithm. Then, VIS enhances the contrast of the rail image. At last, VIS detects defects using the defect localization based on projection profile (DLBP), which identifies possible defects using the projection profile of the mean intensity over each longitudinal (or transversal) line. This is robust to noise and very fast. The proposed LN method and DLBP algorithm are better than the related well-established approaches. The distance of the crack can also be found based on certain assumption.

**Keywords:** Discrete surface defects, local normalization (LN), projection profile, visual inspection.

---

### I. INTRODUCTION

RAIL inspection is an important task in railway maintenance. The speed and loads of trains have been increasing greatly in recent years, and these factors inevitably raise the risk of producing rail defects. For the safe operation of railway systems, the quality of rails must be closely and frequently monitored. The detection of cracks in rails is a challenging problem, and much research effort has been spent in the development of reliable, repeatable crack detection methods for use on in-service rails. While crack detection in the rail head and shear web is reliably achieved using ultrasonic and eddy current methods, neither technique is particularly effective for the detection of cracks in the rail foot. The results of these studies confirm the ability of the proposed method to locate and quantify surface-connected notches and cracks.

Rail defect detection has highly concerned railway operators, and related techniques have been improved greatly in last decades. Traditionally, rail defects were inspected manually by a trained person who views rails visually. Human inspection, however, is slow, subjective, and dangerous. The limitation of human inspection led to many advanced nondestructive testing (NDT) techniques, which acquire the condition of a rail by certain sensors (such as visual and ultrasonic sensors) and then detect defects with sophisticated software.

Nowadays, available NDT techniques for rail inspection include the use of visual cameras, ultrasonics, eddy current, etc. Recent surveys of NDT of rails can be found. Ultrasonic inspection has the best performance for detecting internal cracks. However, its inspection speed is slow (no more than 75 km/h); furthermore, it cannot detect surface defects. Several improved ultrasonic techniques were proposed to increase the inspection speed, such as electromagnetic acoustic transducers, lasers, and air-coupled ultrasonic, but they did not achieve enough progress to detect surface defects. Eddy current testing identifies defects using magnetic field generated by eddy currents. It has relatively high inspection speed and is able to detect surface defects, so it is widely combined with ultrasonics for rail inspection. However, the sensor of eddy current is so sensitive to the lift-off variation that the probe should be positioned at a constant distance (no more than 2 mm) from the surface of the rail head. As a result, the operation of eddy current testing is complex and sensitive; furthermore, the reported highest speed of this testing is also no more than 100 km/h.

Visual inspection has been developed in recent years with the great progress of computer vision techniques. In a visual inspection system (VIS), a high speed digital camera, which is installed under a test train, is used to capture images of a rail track as the train moves over the track, and then, the obtained images are

analyzed automatically using a customized image processing software. Typical applications include bolt detection, corrugation inspection, and crack detection. Visual inspection has the advantages of high speed, low cost, and appealing performance and is regarded as the most attractive technique for surface defect detection. This paper focuses on the core techniques of VIS and presents a real-time VIS for discrete surface defects of rail heads. The rest of this paper is organized as follows. Section II describes the challenges to face. Section III describes the overview of VIS. Section IV introduces the LN method, and Section V presents the DLBP algorithm. Finally, Section VI provides the conclusions and suggests the possible future investigations. Section VII gives the References.

## **II. CHALLENGE OF DETECTING DISCRETE SURFACE DEFECTS**

Rail surface defects are roughly divided into two categories: corrugations and discrete defects. Corrugations are rail head defects that appear on the surface of a rail head in a repeatable or periodic manner. Discrete defects appear on the surface of a rail head in a random or arbitrary manner, i.e., without any characteristics of repeatability. Discrete defects are difficult to be detected for a VIS because of the following factors.

### **1) Limited features available for recognition.**

Discrete defects do not share common texture or shape features, unlike the corrugations that have periodic texture features. The most reliable feature to distinguish discrete defects from background is local gray-level information. The limitation of visual features makes inspection systems exclude most object recognition methodologies that are based on sophisticated texture and shape features.

### **2) Illumination inequality.**

Rail images are captured by a camera installed under a moving test train in an open circumstance. The setup of the image acquisition system used in this work is shown in fig. The illumination in an image is ready to be changed because of natural light and the shake of the train.

### **3) Variation of reflection property of rail surfaces.**

The surface of a rail head does not always share the same reflection property. For example, the center region is often smooth and reflects more light by specular reflection, whereas some areas of periphery may be covered with rust and reflects less light by diffuse reflection. Of course, defects are coarse and reflect less light by diffuse reflection.

### **4) Requirement of high detection speed.**

Inspection systems are expected to be in real time in high-speed railway systems, so a preferable inspection system should have a low computational complexity. In ideal conditions, the gray level of defects is lower than that of back ground (defect-free areas); however, this order is often broken by illumination inequality and the variation of reflection property of rail surfaces. This disorder of gray level between defects and background brings out challenges for VISs.

## **III. OVERVIEW OF WORK**

This paper presents a real-time VIS for discrete surface defects of rail heads. VIS comprises the image acquisition subsystem (IAS) and the image analysis subsystem. IAS acquires gray rail images for the surface of a rail head and the latter processes rail images and detects possible defects. In this paper, i focus on two key techniques of VIS: contrast enhancement and defect localization. I propose the local normalization (LN) method to enhance the distinction between defects and background in a rail image, considering illumination inequality and the variation of reflection property of rail surfaces.

In addition, i put forward the defect localization based on projection profile (DLBP) algorithm, which identifies possible defects using the projection profile of the mean intensity over each longitudinal (or transversal) line. In addition to this the distance to the crack is also identified.

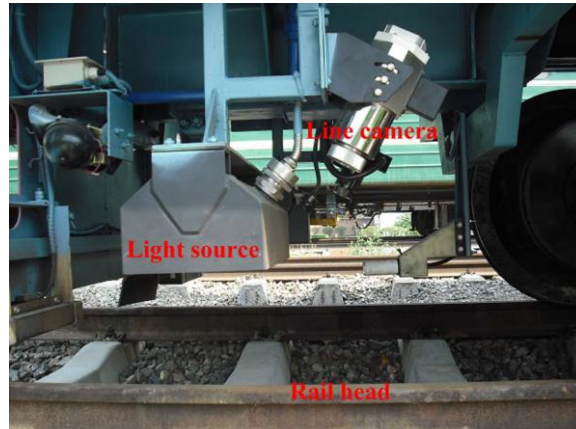


**Figure 1:** Diagram of image acquisition system

**VIS has the following advantages:**

- 1) LN is nonlinear and illumination independent. Therefore, it is able to eliminate the illumination inequality of rail images. In addition, it can greatly reduce the variation in the background of a rail image.
- 2) DLBP is fast and robust to noise, because DLBP relies on the local distribution of intensities, rather than global characteristics used in most thresholding algorithms
- 3) VIS is very fast with a linear computational time complexity. Under our experimental setup, VIS is able to be in real time with a speed of 216 km/h, which is greatly faster than that of ultrasonic and eddy current inspection.

VIS includes two parts: IAS and image analysis subsystem. IAS captures series of images of a rail surface, and the latter is designed to detect defects from the images generated by IAS.

**A. IAS**

IAS is made up of several commercially available components. The basic component is a Dalsa Spyder 2 line-scan camera, which has 1024 pixels of resolution and a maximum line rate of 65 000 lines/s. A PC-CamLink frame grabber is utilized to capture rail images based on the Cameralink protocol. An illumination setup equipped with four LED light sources is installed in order to reduce the effect of natural light. Moreover, the line-scan camera is triggered by a wheel encoder to synchronize data acquisition. This trigger sets the pixel resolution along longitudinal direction Y (or motion direction) at 1 mm. The resolution along the transversal direction X is also 1 mm. The size of each generated rail image is 1200×512 (1200 pixels in Y and 512 pixels in X). The IAS is installed under a test train as in Fig. I have to note that the quality of rail images captured by IAS is inevitably affected by natural light and the shake of the train.

**B. Framework of Image Analysis Subsystem**

After a rail image is generated by the IAS, it is processed by the image analysis subsystem, which aims to efficiently detect possible defects in the image. This subsystem includes three main modules: rail track extraction, contrast enhancement, and defect localization. Fig shows the diagram of the subsystem.

**1) Rail track extraction.** A rail image obtained by the IAS includes extra fields besides the rail track, as shown in Fig. Therefore, the region of the rail track should be first extracted in order to reduce the area to be inspected in the subsequent procedures. I put forward the algorithm called track extraction based on projection profile (TEBP). TEBP is supported by the observations: 1) Rail tracks have fixed width

**2) Rail tracks have higher average intensity in each longitudinal line compared with extra fields.**

TEBP algorithm first computes the projection profile of mean intensity over each longitudinal line in a rail image and then searches the fixed-length interval that has the maximum accumulative value of the profile. The interval with the maximum value finally determines the position of a rail track. The TEBP algorithm is described in algorithm.

### Algorithm

```
1: procedure TEBP(srcImg, railWidth)
2: rows ← size(srcImg, 1) _ Longitudinal direction
3: cols ← size(srcImg, 2) _ Transversal direction
4: H(1) ← mean of srcImg( · , 1)
5: for i ← 2, cols do
6: H(i) ← mean of srcImg( · , i)
7: H(i) ← H(i) + H(i - 1) _ Cumulative value
8: end for
9: maxCum ← -1
10: pBegin ← 0
11: for i ← 1, cols - railWidth + 1 do
12: curCum ← H(i + railWidth - 1) - H(i)
13: if curCum > maxCum then
14: maxCum ← curCum
15: pBegin ← i
16: end if
17: end for
18: return pBegin
19: end procedure
```

**2) Contrast enhancement:** Defects are easy to be hidden or confused in rail images because of illumination inequality and the variation of reflection property of rail surfaces, so contrast enhancement is a necessary procedure to highlight defects from their background. I propose the LN method to enhance the distinction between defects and their background. In this method, a rail image is divided into several nonoverlapped windows, and each pixel in a window is normalized by the mean and standard deviation of the window. The normalized image is further enhanced by a defect-proportion limited filter.

The LN method has two notable advantages:

- 1) Normalized images are illumination independent
- 2) It obtains a homogeneous background and highlights defects.

**3) Defect localization:** A normalized image comprises three types of pixels: defects, background, and noise. Defects are spatially clustered with low intensity, background is spatially uniform with high intensity, and noise is randomly distributed for both space and intensity. Taking the spatial distribution and intensity property into account, I put forward the DLBP algorithm. In this method, the longitudinal suspect positions (or intervals) of defects are first located by analyzing the projection profile of the mean intensity of each transversal line. Each longitudinal suspect interval (LSI) determines a subimage. Then, transversal suspect positions are obtained based on the transversal profile in the subimage. Finally, each pair of longitudinal and transversal intervals forms a suspect rectangle (SR), and the rectangle is recognized as defects or background by a thresholding rule. DLBP is not only fast but also robust to noise.

## IV. LOCAL NORMALIZATION

The quality of rail images captured by IAS is easy to be degraded because IAS suffers from the influence of natural light and the shake of the test train. Furthermore, the quality is also affected by the reflection property of rail surfaces. For example, smooth parts reflect more light by specular reflection, whereas coarse regions reflect less light by diffuse reflection. Based on these considerations, I propose the LN to improve the quality of rail images.

In this section, I first describe the approximate model of image formation of IAS and then present the LN method. Finally, I propose the defect-proportion-limited filter to further enhance normalized images. Contrast enhancement is important for image processing, particularly in industrial applications. There are many well-established approaches, such as global histogram equalization (GHE), local histogram equalization, and adaptive contrast enhancement. It's believed that a contrast enhancement algorithm for rail images should consider the following facts:

- 1) Large-intensity variation of background in global scope. The background, globally considered in a rail image, often has a large dynamic intensity range because of the difference in illumination and reflection property of the rail surface. For example, natural light (particularly, the sunlight) may change the local illumination condition; smooth parts of a rail surface reflect more light than coarse parts. The intensity of background ranges from the highest value to the almost lowest value.
- 2) Small-intensity variation in local regions. In a local window, for example, a longitudinal line, the illumination and reflection property are ready to be stable, so the local window tends to have small variation.
- 3) Disorder of gray level between defects and background. Generally speaking, the intensity of defects is less than that of background. However, this order can be changed because of variations of illumination and reflection property. For example, some rust like pixels in Fig have smaller or equivalent gray values compared with the defect pixels. Based on these considerations, I propose the LN method inspired by the similar techniques for face recognition. Supposing a  $w \times h$  window  $W$  and a related pixel  $(x, y)$ , the intensity of the pixel is transformed by

$$L(x, y) = \frac{F(x, y) - E(x', y')}{\text{var}(F(x', y'))}, (x', y') \in W$$

where  $E(\cdot)$  is the mean of  $F(x', y')$  in  $W$  and  $\text{Var}(\cdot)$  is the corresponding standard variance. Note that a small constant is added to the variance in implementation in order to avoid dividing by zero. The transformed image  $L$  is called local normalized image (LNI). LNI has the following properties, which will be of benefit to defect detection.

#### **Defect-proportion-limited filter**

LNIs can be further enhanced if its considered for the following two facts. First, the proportion of defects is always small for a railway in service, since discrete defects do not have large area and occur with a small probability. Second, intensity of defects is less than that of defect-free pixels in an LNI, but the intensity range of defect-free pixels is relatively large. Therefore, I further enhance an LNI by a defect-proportion-limited filter. Given the upper bound of defect proportion  $dp$ , a threshold  $T_{dp}$  is determined by

$$T_{dp} = \text{argmin}(|\frac{\text{Num}(L(x, y) < T)}{\text{Num}(L)} - dp|)$$

where,  $\text{Num}(L(x, y) < T)$  denotes the number of pixels that have smaller intensity than 'T' and  $\text{Num}(L)$  is the total pixel number in 'L'. Note that threshold  $T_{dp}$  can be fast estimated based on the histogram of  $L$ . The threshold  $T_{dp}$  divides the pixels of LNI into two groups:  $C_0 = L(x, y) < T_{dp}$  and  $C_B = L(x, y) \geq T_{dp}$ .  $C_0$  consists of both defects and background, whereas  $C_B$  only comprises background.

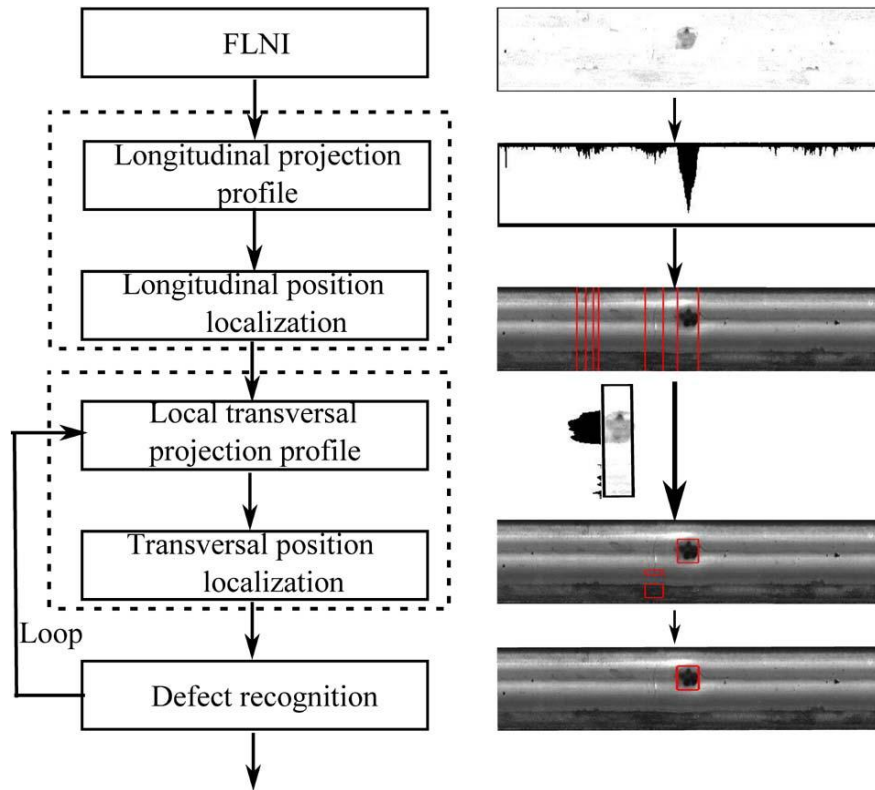
After the threshold  $T_{dp}$  is obtained,  $C_B$  is truncated with  $T_{dp}$  to reduce the intensity range of background. Consequently, the filtered LNI (FLNI) can be derived

$$FL(x, y) = \begin{cases} L(x, y) & \text{if } L(x, y) < T_{dp} \\ T_{dp} & \text{otherwise} \end{cases}$$

Fig. shows the FLNIs with  $dp$  taking 0.4, 0.3, and 0.1, respectively. We can observe that FLNIs have better contrast and preserve the necessary information of defects. FLNIs are normalized to the integer range  $[0, 255]$  for the next processing.

### **V. DEFECT LOCALIZATION (DLBP)**

There are three types of pixels in an FLNI: background, defects, and noise. In the quantitative aspect, pixels of defects and noise take lower gray values than those of background; furthermore, defects fall in a narrow and low gray interval, whereas noise ranges widely. In the spatial aspect, pixels of a defect are spatially clustered together, but noise and background are almost uniform.



## 2. Framework of DLBP algorithm

As a consequence, the mean of gray value on a transversal line will be small if the line crosses a defect. Similarly, the mean on a longitudinal line in a local window will also be small if the line passes through a defect. Thereby, I put forward the DLBP algorithm. Fig shows the framework of DLBP algorithm, which includes three main procedures: longitudinal position localization, transversal position localization, and defect recognition. The first procedure analyzes the projection profile of mean intensity of each transversal line and locates LSIs. The second one locates transversal suspect interval (TSI) in the local subimage determined by an LSI. The final procedure recognizes each SR constructed by an LSI and TSI pair.

### A. Longitudinal Position Localization

Given FL, the mean intensity  $m_y$  of a transversal line  $Y = y$  is given by

$$m_y = \sum_x FL_{(x,y)} / NX$$

where  $NX$  denotes the length of FL in the transversal direction. Note that the axis of  $X$  refers to the transversal direction and  $Y$  is the longitudinal direction in this work. In order to highlight the positions referring to defects, we define the longitudinal projection profile  $HY$  as  $Hy = 255 - my$ ,  $y \in [1, NY]$ , where  $NY$  denotes the length of FL in the longitudinal direction  $Y$ . Fig. 3(b) shows  $HY$  of the FLNI in Fig. 3(a). From Fig. 3(b), we can observe that the defect is highlighted although the FLNI is somewhat noisy. Longitudinal positions of suspect defects are located with four procedures based on  $HY$ .

- 1) The profile  $HY$  is filtered by a high-pass filter, in which the cutoff value is set as the mean  $\mu_Y$  of  $HY$ . If  $Hy$  for  $y \in [1, NY]$  is less than  $\mu_Y$ , then  $Hy$  is set to zero.

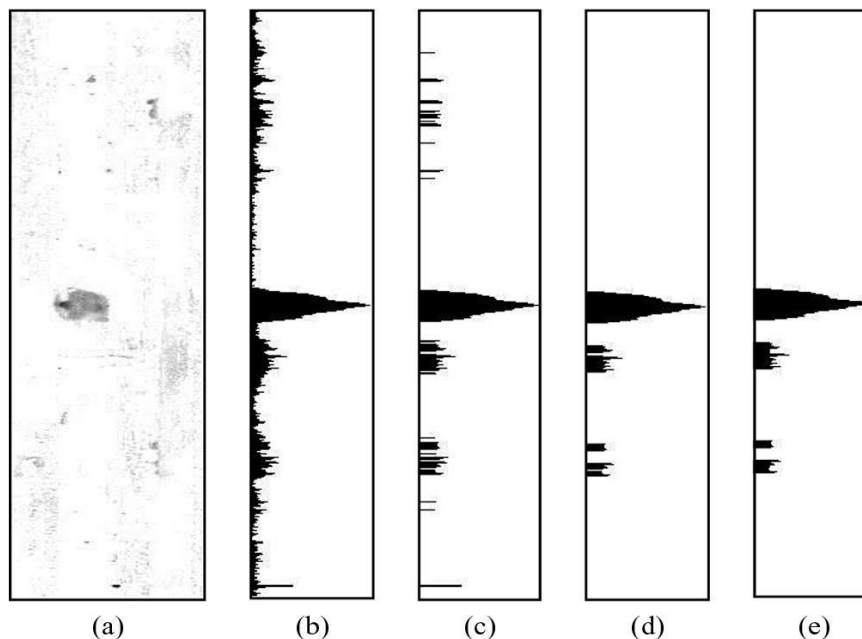


**Fig.3** Processing of longitudinal position localization. (a) FLNI. (b) Projection profile on longitudinal direction. (c) Filtered profile. (d) Smoothed profile.(e) Concatenated profile.

Otherwise,  $H_y$  keeps the original value. Fig. 3(c) shows the filtered profile, which comprises many intervals. Narrow intervals are mostly caused by noise and are smoothed by the next procedure.

2) The filtered profile is smoothed to eliminate narrow intervals. Set the minimum length of retained intervals as  $\Delta$ . If the length of an interval is less than  $\Delta$ , then  $H_y$  in the interval is set to zero. Otherwise, the interval is not changed.  $\Delta$  is set as five in this study. Fig. 3(d) shows the smoothed result of Fig. 3(c).

3) The smoothed profile is concatenated to reduce the risk of over segmentation. Neighboring intervals with small gap are merged together. The minimum gap between two neighboring intervals is set as three. Fig. 3(e) shows the concatenated result of Fig. 3(d).

4) Each continuous interval in the concatenated profile is defined as an LSI. We set  $LSI = [Dy1, Dy2]$  where  $Dy1$  and  $Dy2$  denote the low and high coordinates of the LSI in the axis  $Y$ , respectively.

### B. Transversal Position Localization

Transversal positions of defects are located with similar method as LSI, except that the profile here is defined on the transversal direction and computed in a subimage determined by an LSI. First, the subimage crossing the LSI ( $LSI = [Dy1, Dy2]$ ) is cropped, and then, the local transversal projection profile  $H_x$  is computed as

$$H_x = 255 - \sum_{y \in [Dy1, Dy2]} FL_{(x,y)} / (Dy2 - Dy1 + 1)$$

Fig. 4(a) and (b) shows an example of such subimage and its  $H_x$ , respectively. Second,  $H_x$  is filtered, smoothed, and concatenated sequentially, just as  $H_y$ . Fig. 4(c) and (d) shows the corresponding results. Finally, each continuous interval is defined as a TSI, and we set  $TSI = [Dx1, Dx2]$  where  $Dx1$  and  $Dx2$  denote the low and high coordinates of TSI in the axis  $X$ , respectively.

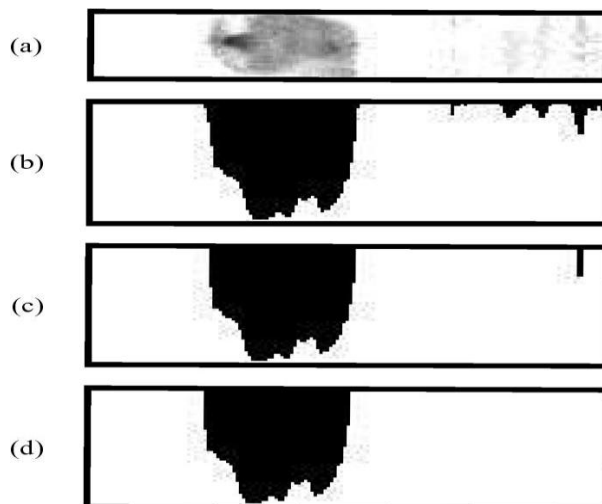


**Fig.4.** Processing of transversal position localization. (a) Local FLNI. (b) Projection profile on transversal direction. (c) Filtered profile. (d) Profile after smoothing and concatenation.

### C. Defect Recognition

An SR will be determined after a matched LSI and TSI pair is obtained, denoted as  $SR = [Dy1 : Dy2, Dx1 : Dx2]$ . Some SRs, however, are not true defects due to noise. So, each SR should be further checked. An SR is identified as a defect or not by two features: area and regional contrast. In one aspect, the area of a defect, according to the standard of railway maintenance, should be greater than a minimum value. Therefore, the SR is first judged with an area threshold  $T_a$ . In the other aspect, a defect has a notable contrast to its neighborhood, particularly in the longitudinal direction. We consider the extended rectangle  $ER = [Dy1 - h/2 : Dy2 + h/2, Dx1 : Dx2]$  where  $h$  denotes the extended length in the longitudinal direction and is set as  $h = Dy2 - Dy1$  and calculate the regional contrast  $C$  between SR and ER by

$$C(SR) = \frac{\mu_{ER} - \mu_{SR}}{\mu_{ER}}$$

where  $\mu_{ER}$  and  $\mu_{SR}$  denote the mean gray values of ER and SR in the original rail image, respectively. SR is further judged with a contrast threshold  $T_C$ . As a whole, an SR is identified by the following rule:

$$T(SR) = \begin{cases} 1, & \text{if } Area(SR) \geq T_a \text{ and } C(SR) \geq T_C, \\ 0, & \text{otherwise} \end{cases}$$

where the area threshold  $T_a$  is defined according to the specification of railway maintenance and the resolution of captured rail images, and the contrast threshold  $T_C$  is set as  $T_C = 0.1$  in this paper. Of course, we can add an upper limitation of area to SR if it is needed. Note that there are other sophisticated recognition approaches that can be applied for defect recognition, but we adopt the thresholding method here because of two factors. On the one hand, this method is fast and simple. On the other hand, we would like to focus on the contrast enhancement and defect localization methods in this paper.

I have developed the VIS for discrete surface defects of rail heads. More specially, I put forward the LN method for contrast enhancement of rail images. This method is nonlinear and illumination independent, so it is able to overcome the challenges: illumination inequality and the variation of reflection property of rail surfaces. In addition, I propose the DLBP algorithm to locate defects in a normalized image. DLBP is based on local gray-level distribution and robust to noise. I thoroughly analyze the parameters of VIS and compare the LN method and DLBP algorithm with the related classic methodologies.

In addition to this I prefer to find out the distance from the initial position to the crack inspected frame. In this process the crack from each of the track analyzed and important information like the distance of the track from the initial point and the crack area the centroid of the crack etc are found out. It is based on the assumption that the train has a uniform speed. The assumed speed of train is 20km/hr. The mean detection time for a rail image is no more than 20 ms. An image covers 1.2 m of a rail under the setup of the IAS. Accordingly, we can derive that the average detection speed of VIS is about 216 km/h, which is far higher than that of

ultrasonic inspection (up to 75 km/h) and eddy current testing (up to 100 km/h) which is implemented in real-time. Here, firstly the set of data having images is considered, from which each image is analysed. An image covers 1.2 m of a rail under the setup of the IAS. When the image having crack is encountered, the distance of the frame from the initial position and the frame number is calculated and displayed. Thereby finding the elapsed time, time taken to process etc.. is found from this. A frame grabber hardware is additionally fit to the train so that it can hold on the images and store them to the memory availing it to the future processing as the time avails.

## VI. CONCLUSION

We have developed the VIS for discrete surface defects of rail heads. More specially, we put forward the LN method for contrast enhancement of rail images. This method is nonlinear and illumination independent, so it is able to overcome the challenges: illumination inequality and the variation of reflection property of rail surfaces. In addition, we propose the DLBP algorithm to locate defects in a normalized image. DLBP is based on local gray-level distribution and robust to noise. We thoroughly analyze the parameters of VIS and compare the LN method and DLBP algorithm with the related classic methodologies. Furthermore, VIS is a very fast system with a linear computational time complexity, and it can be in real time to run on a 216-km/h test train under our experimental setup.

## REFERENCES

- [1]. Qingyong Li, Member, IEEE, and Shengwei Ren, "A Real Time Visual Inspection System For Discrete Surface Defects of Rail Heads", *IEEE transactions on instrumentation and measurement*, vol. 61, no. 8, August 2012.
- [2]. R. Clark, "Rail flaw detection: Overview and needs for future developments," *NDT & E Int.*, vol. 37, no. 2, pp. 111–118, 2004.
- [3]. R. Clark, S. Singh, and C. Haist, "Ultrasonic characterisation of defects in rails," *Insight*, vol. 44, no. 6, pp. 341–347, 2002.
- [4]. R. Edwards, S. Dixon, and X. Jian, "Characterisation of defects in the railhead using ultrasonic surface waves," *NDT & E Int.*, vol. 39, no. 6, pp. 468–475, 2006.
- [5]. M. Bentoumi, P. Aknin, and G. Bloch, "On-line rail defect diagnostics with differential eddy current probes and specific detection processing," *Eur. Phys. J. Appl. Phys.*, vol. 23, no. 3, pp. 227–233, 2003.
- [6]. H. Thomas, T. Heckel, and G. Hanspach, "Advantage of a combined ultrasonic and eddy current examination for railway inspection trains," *Insight-Non-Destructive Testing and Condition Monitoring*, vol. 49, no. 6, pp. 341–344, 2007.
- [7]. F. Marino, A. Distanto, P. Mazzeo, and E. Stella, "A real-time visual inspection system for railway maintenance: automatic hexagonal-headed bolts detection," *IEEE Trans. Syst., Man, Cybern. C, Appl. Rev.*, vol. 37, no. 3, pp. 418–428, May 2007.
- [8]. C. Mandriota, M. Nitti, N. Ancona, E. Stella, and A. Distanto, "Filterbased feature selection for rail defect detection," *Mach. Vis. Appl.*, vol. 15, no. 4, pp. 179–185, 2004.
- [9]. J. Lin, S. Luo, Q. Li, H. Zhang, and S. Ren, "Real-time rail head surface defect detection: A geometrical approach," in *Proc. IEEE Int. Symp. Indust. Electron.*, 2009, pp. 769–774.
- [10]. F. Marino and E. Stella, "ViSyR: A vision system for real-time infrastructure inspection," in *Vision Systems: Applications*, G. Obinata and A. Dutta, Eds. I-Tech, 2007, pp. 113–144.
- [11]. U. Zerbst, K. Madler, and H. Hintze, "Fracture mechanics in railway applications—an overview," *Eng. Fracture Mech.*, vol. 72, no. 2, pp. 163–194, 2005.
- [12]. N. Nacereddine, M. Hamami, and N. Oucief, "Non-parametric histogram based thresholding methods for weld defect detection in radiography,"
- [13]. *World Acad. Sci., Eng. Technol.*, vol. 9, pp. 213–217, 2005.
- [14]. H. Ng, "Automatic thresholding for defect detection," *Pattern Recognit. Lett.*, vol. 27, no. 14, pp. 1644–1649, 2006.
- [15]. B. Phong, "Illumination for computer generated pictures," *Commun. ACM*, vol. 18, no. 6, pp. 311–317, 1975.
- [16]. T. Whitted, "An improved illumination model for shaded display," *Commun. ACM*, vol. 23, no. 6, pp. 343–349, 1980.